Accepted Manuscript

Direct imaging of the dissolution of salt forms of a carboxylic acid drug

Kofi Asare-Addo, Karl Walton, Adam Ward, Ana-Maria Totea, Sadaf Taheri, Maen Alshafiee, Nihad Mawla, Antony Bondi, William Evans, Adeola Adebisi, Barbara R. Conway, Peter Timmins

Please cite this article as: K. Asare-Addo, K. Walton, A. Ward, A-M. Totea, S. Taheri, M. Alshafiee, N. Mawla, A. Bondi, W. Evans, A. Adebisi, B.R. Conway, P. Timmins, Direct imaging of the dissolution of salt forms of a carboxylic acid drug, *International Journal of Pharmaceutics* (2018), doi: https://doi.org/10.1016/j.ijpharm.2018.09.048

Direct imaging of the dissolution of salt forms of a carboxylic acid drug

Kofi Asare-Addo[a]*, Karl Walton[b], Adam Ward[a], Ana-Maria Totea[a], Sadaf Taheri[a], Maen Alshafiee[a], Nihad Mawla[a], Antony Bondi[a], William Evans[a], Adeola Adebisi[a], Barbara R. Conway[a], Peter Timmins[a]

[a]Department of Pharmacy, University of Huddersfield, Huddersfield, HD1 3DH, UK

[b]EPSRC Future Metrology Hub, University of Huddersfield, Huddersfield, HD1 3DH, UK

*Corresponding author (Kofi Asare-Addo)

e-mail: k.asare-addo@hud.ac.uk

Tel: +44 1484 472360

Fax: +44 1484 472182

Abstract

The optimisation of the pharmaceutical properties of carboxylic acid drugs is often conducted by salt formation. Often, the salt with the best solubility is not chosen due to other factors **such as stability, solubility, dissolution and bioavailability** that are taken into consideration during the preformulation stage. This work uses advanced imaging techniques to give insights into the preformulation properties that can aid in the empirical approach often used in industry for the selection of salts. Gemfibrozil (GEM) was used as a model poorly soluble drug. Four salts of GEM were made using cyclopropylamine (CPROP), cyclobutylamine (CBUT), cyclopentylamine (CPENT) and cyclohexylamine (CHEX) as counterions. DSC, XRD and SEM were used to confirm and characterise salt formation. IDR obtained using UV-imaging up to 10 min for all the salts showed that an increase in the chain length of the counterion caused a decrease in the IDR. Past the 10 min mark, there was an increase in the IDR value for the CPROP salt, which was visualised using UV-imaging. The developed interfacial (surface) area ratio (Sdr) showed significant surface gains for the compacts. Full dosage form (capsule) imaging showed an improvement over the GEM for all the salts with an increase in chain length of the counterion bringing about a decrease in dissolution which correlated with the obtained UV-imaging IDR data.

developed interfacial (surface) area ratio; USP, United States pharmacopeia; **IDR, intrinsic dissolution rate**

1. Introduction

Poor aqueous solubility, which is now typical of the majority of emerging active pharmaceutical ingredients (API), can be a challenge in pharmaceutical development (Al-Hamidi et al., 2010a; Korn and Balbach, 2014; Ku and Dulin, 2012; Williams et al., 2013). As a result of their crystal structures, APIs can also have undesirable properties which can impact their physicochemical and mechanical properties thus affecting compaction, dissolution, bioavailability, hygroscopicity and stability to name a few (Asare-Addo and Conway, 2017; David et al., 2010; Ramirez et al., 2017). Many of these NCEs belong to the Biopharmaceutical Classification System (BCS) class II and are characterized by their high membrane permeability and low aqueous solubility; the rate and extent of absorption of these drugs from the gastrointestinal tract (GIT) is thus dependent on their solubility and dissolution rate (Amidon et al., 1995).

Common methods used in overcoming the poor solubility of these APIs include particle size reduction, complexation, using additives in crystallization, cocrystals, liquisolid techniques and salt formation (Adebisi et al., 2016a; Adebisi et al., 2016b; Al-Hamidi et al., 2014, 2013, 2010a, 2010b; Asare-Addo et al., 2015; Nokhodchi et al., 2005; Rabinow, 2004; Stahl et al., 2008).

A salt formation involves an acid/base reaction that involves neutralisation or a proton transfer making the drug molecule forming strong ionic interactions with a counterion that is oppositely charged (Berge et al., 1977; Stahl and Wermuth, 2011)**.** Salt formation **is usually the first consideration and** remains an effective and widely used technique for improving the solubility, physicochemical and mechanical properties of ionisable drugs **such as poor stability, physical quality, purity, optimising process chemistry, reducing toxicity and altering the absorption in the gastrointestinal tract** (He et al., 2017; Stahl et al., 2008). **Salt formation is also the preferred option regarding the solubility enhancement of drug molecules when compared**

3

to co-crystals and polymorphs (Pindelska et al., 2017)**. Tsutumi et al. evaluated the use of miconazole salts on the physiochemical properties of the drug. Intrinsic dissolution tests were carried out to compare the dissolution rates of maleate, hemifumarate, hemisuccinate, nitrate and the free base and the authors found the miconazole salts showed approximately 2-2.5 times higher dissolution rate than the free base** (Tsutsumi et al., 2011)**.** Supuk et al. observed that the choice of counterion for flurbiprofen salts significantly impacted its morphology, electrostatics and tabletability (Šupuk et al., 2013). David et al. compared the physical, mechanical and crystallographic properties of a series of gemfibrozil salts (David et al., 2012). The authors found that salt formation increased the aqueous solubility of gemfibrozil and that solubility increased with the number of hydroxyl groups on the counterion. They observed that the increased capacity for hydrogen bond formation had an influence on the crystal structure of the salt and that the increasing hydrophilicity of the counterion was beneficial in solubility enhancement. Ramirez et al. characterised the crystal packing, chain conformation and physiochemical properties of crystalline gemfibrozil amine salts (Ramirez et al., 2017). They observed that the cyclic amine counterions increased the melting point, which correlated with an increase in counterion molecular weight whereas the linear amine counterions had a decrease in melting point with an increasing molecular weight **and volume**. Yang et al. explored the structure-property relationship of three diamine gemfibrozil salts. Thermal analysis showed an increase in melting point with the use of the counterion. **The three salts showed an increased dissolution rate compared** to that of the free acid (Yang et al., 2016).

An important parameter determined in early stage drug development is intrinsic dissolution rate (IDR) as it may help to predict API behaviour *in vivo*. **Intrinsic dissolution is a feasible alternative to equilibrium solubility to determine the BCS class and has several advantages, especially with respect to time, quantity of material, and handling of samples. Drugs with an intrinsic dissolution rate above 0.1 mg min^{-1}cm^{-2} would be considered highly soluble, and rates**

4

below this limit would indicate drugs with low solubility. The Surface Dissolution Imaging (SDI2) instrument (Pion-Inc, UK) allows the study of real-time surface and whole dosage form. This is version 2 of the SDI instrument with Actipix™ Technology from Sirius Analytical, UK now Pion Inc). The SDI instrument has been used extensively in characterising the IDRs of APIs as well as in other applications and **requires little sample** (Boetker et al., 2013; Gordon et al., 2013; Hulse et al., 2012; Niederquell and Kuentz, 2014; Nielsen et al., 2013; Østergaard et al., 2014). Ward et al. recently used a range of advanced imaging techniques to assess the surface properties of ibuprofen compacts used in an SDI study to determine IDR (Ward et al., 2017). X-ray powder diffraction (XRPD) and differential scanning calorimetry (DSC) showed no changes in the crystal structure of ibuprofen after compaction and SDI testing. Variable-focus microscopy revealed changes in the surface topography of the compacts that impacted IDR measurement.

The choice of counterion for salt formation has a great impact on selection for drug development, the objectives of this research was to prepare and characterise four salts of the poorly soluble anti-hyperlipidaemia drug gemfibrozil (GEM) (Figure 1a) using a structurally-related series of counterions; cyclopropylamine (CPROP), cyclobutylamine (CBUT), cyclopentylamine (CPENT) and cyclohexylamine (CHEX) (Figure 1b-e). The authors aim to use a focus variation microscope to give insights to how the effects of the counterions potentially impact the topography of the compacts pre-IDR run on the novel SDI2 instrument and to understand how that impacts on determined IDR. In a development to the previous instrument, the SDI2 can image whole dosage forms and this was used to study the impact of the salt-form on drug release and imaging from **hard gelatine** capsules.

2. Materials and Methods

2.1. Materials

5

GEM was purchased from Sigma-Aldrich (UK). The counterions - CPROP, CBUT, CPENT and CHEX used in the preparation of the salts were all of analytical grade and purchased also from Sigma-Aldrich (UK). **Although the counterions used in this experimentation are cyclic molecules, the term "chain length" is used to define the increase in carbon chain length for simplicity in the rest of the manuscript.** Acetonitrile and ethanol, the solvents used in the preparation of the salts were of analytical grade purchased from Fisher (UK). The media used for IDR determination and whole dosage imaging was phosphate buffer (pH 7.2) prepared according to the USP 2003 using sodium hydroxide and potassium phosphate monobasic purchased from Fisher (UK) and Acros Organics (Germany) respectively.

2.2. Salt preparation

The salts were prepared as reported by Ramirez et al. (Ramirez et al., 2017). In brief, equimolar ratios of the drug (GEM) and counterion (CPROP, CBUT, CPENT and CHEX) were dissolved in 50 mL of acetonitrile and the resultant precipitated salt filtered under vacuum. The recovered salts were re-crystallised from methanol after which they were dried at 50 °C for up to 12 h. All the salts produced were then sealed in glass vials and stored until required.

2.3. Solid State characterisation

2.3.1. Scanning electron microscopy (SEM)

A scanning electron microscope (**JSM-6060CV SEM, JEOL Inc, MA, USA**) operating at 10 kV was used to obtain electron micrographs. Before observation, each of the samples (GEM and its salts with CPROP, CBUT, CPENT and CHEX) was mounted on a metal stub with double-sided adhesive tape and sputter-coated with an ultra-thin coating of gold/palladium (80:20) for 60 s using

6

a Quorum SC7620 Sputter Coater under vacuum with gold in an argon atmosphere. To aid the study of the morphology of the salts, micrographs with different magnifications were taken.

2.3.2. Differential scanning calorimetry (DSC)

The enthalpy, onset temperatures and melting points of GEM, and its salts with CPROP, CBUT, CPENT or CHEX were obtained using the software provided by Mettler-Toledo, Switzerland. This was done by first placing about 3-6 mg of GEM, or its salts with CPROP, CBUT, CPENT and CHEX in standard aluminium pans (40 µL) with a vented lid. The crimped aluminium pans were heated from 20 to 250 ˚C at a scanning rate of 10 °C/min using nitrogen gas as a purge gas in a DSC 1 (Mettler-Toledo, Switzerland).

2.3.3. X-ray powder diffraction (XRPD)

GEM and its salts with CPROP, CBUT, CPENT and CHEX were scanned in Bragg–Brentano geometry, over a scattering (Bragg, 2θ) angle range from 5 to 100°, in 0.02° steps at 1.5° min^{-1} using a D2 Phaser diffractometer (Bruker AXS GmbH, Karlsruhe, Germany) (Laity et al., 2015). The XRPD patterns were collected and analysed further using Microsoft Excel.

2.4. Surface analysis using a focus variation microscope (FVI) and intrinsic dissolution rate (IDR) determination

Compacts for IDR were produced by using 10 mg of either GEM or its salts with CPROP, CBUT, CPENT and CHEX at a compression force of **980 N or 0.98 kN** using a hand-crank press (Pion Inc). Prior to IDR determination, surface assessment of the compacts for IDR was undertaken to determine the effect of the counterions on the developed interfacial (surface) area ratio (Sdr) of the compacts over the parent drug GEM. The true surface area of the textured sample compared to that of a uniform flat surface is known as the Sdr. It is expressed as a percentage by which the true

7

measured surface area exceeds that of the nominal uniform measurement area (Equation 1). The focus variation microscope Alicona™ microscope (Alicona Imaging GmbH, Graz, Austria) was used for this determination as previously reported by Ward et al. (Ward et al., 2017). Surfstand™ software (Taylor Hobson, UK, and University of Huddersfield, UK) was used to analyse the images. The SDI2 (Pion Inc) was used in the determination of IDR. The nominal surface area of the compact is taken into consideration with the way the software calculates IDR values. The molar extinction coefficient of the dissolved GEM was experimentally determined using a range of GEM concentrations in phosphate buffer (pH 7.2). The dissolution media (pH 7.2) was maintained at 37 °C and used for UV-imaging and determination of IDR at a flow rate of 2 mL/min for 30 min . All experiments were conducted in triplicate and at a wavelength of 280 nm for the dissolved GEM.

$$Sdr = \frac{(Texture\ Surface\ Area) - (Cross\ Sectional\ Area)}{Cross\ Sectional\ Area}$$
Equation 1

2.5. Whole dosage form dissolution

Capsules containing 150 mg of GEM **(powder – used as from Sigma-Aldrich)** or salts **(formulation powder produced as used from section 2.2)** equivalent to 150 mg GEM content were prepared using size 0 hard gelatine capsules. These samples were then mounted using a wire holder (Figure 2a) and placed within the sample holder (Figure 2b). The whole dosage cell was inserted and connected to the fluid lines. The experiment was conducted using phosphate buffer (pH 7.2) maintained at 37 °C at a flow rate of 8.2 mL/min. The release of GEM was imaged at various time points over a period of 60 min at a wavelength of 280 nm. All experiments were conducted in triplicate.

3. RESULTS AND DISCUSSION

3.1. Solid-state analysis

DSC showed GEM to have a melting point of 60.3 °C. This was **a sharp narrow peak** similar to that published by Ramirez et al. (Ramirez et al., 2017) **and Aigner et al.** (Aigner et al., 2005) who reported a melting temperature of 61.2 **°C and 59.3** °C **respectively**. **The single endotherm confirmed the thermal stability of GEM and thus the absence of polymorphism within GEM.** The melting points for the CPROP, CBUT, CPENT and CHEX salts are recorded in Table 1. The CBUT and CHEX salts are also in direct agreement with data previously published however, the CPROP salt melt was about 5 °C different to that published (Ramirez et al., 2017). All the salts produced were found to be crystalline in nature. **There was also no degradation observed up to the temperature studied. There was also no evidence of any hydrate/solvate formation in all of the salts studied.** XRPD confirmed the characteristic peaks of GEM at **numerous and sharp reflections at** 2θ at 11.6°, 14°, 18° and 24° (Chen et al., 2010) (Figure 3) **showing GEM to be crystalline in nature as expected**. XRPD also showed all the salt made were crystalline in nature (Figure 3). The SEM images are depicted in Figure 4. **The surface morphology of GEM consisted mainly of columnar crystals with rounded edges (Figure 4a). This was observed also by Ambrus et al** (Ambrus et al., 2012)**. The CPROP and CPENT salts were columnar and rod like in shape with the CPROP exhibiting more agglomeration. The CBUT samples were needle-like in morphology whereas the CHEX salts showed a network of fine needles on larger particles.**

3.2. Intrinsic dissolution rate

9

It must be noted that the IDR values reported here were taken after the 5 min mark with the flow cell operating at 0.2 mL/min. Hulse et al. reported using IDR values from a UV imaging technique after the 3 min mark due to potential erroneous measurements as a result of drug particles on the surface (Hulse et al., 2012). In an earlier study conducted by Niederquell and Kuentz, SEM images showed that the APIs studied had uneven surfaces on the IDR discs (Niederquell and Kuentz, 2014). Using a focus variation microscope, Ward et al. reported that loose particulates were indeed at the rim and on the surface of IDR compacts which can give rise to inflated IDR values (Ward et al., 2017). In this current work, we have demonstrated that the **compression** of the compacts influences the surfaces of the compacts which may be as a result of the properties of the materials thereby impacting IDR measurements (Figure 5). Surfstand analysis of GEM compacts at a 5x optical magnification showed that Sdr had a surface gain of up to 10.5 % (Table 1). There was a general decrease of the developed interfacial (surface) area ratio for all the salts compared to the free acid with the exception of the CHEX salt, which had an Sdr value of up to 23 % at the same magnification. This gives a formulator an idea as to how the salts may compact with regards to possible elasticity due to potential elastic recovery or how brittle the salt formed may be due to potential crack on the surface. This is an area of interest, which the authors are currently investigating. The zoom analysis on Figure 5 at the 10 to 50x magnification also shows the rings picked up on the surface of the compacts from the tooling surface as well as individual particulates on the surface of especially GEM and the CPROP salt (highlighted by the black dashed circles in Figure 5). All of these findings highlighted the importance of observing the surface to ensure accurate IDR data is obtained.

Data gathered at the 10 min mark showed GEM to have a poor IDR. Salt formation significantly improved the IDR for all products (Table 1). The data also suggest a potential trend in the IDR values with increasing chain length bringing about a general decrease in IDR. This however is not true for the CPENT salt. It was observed over the 30 min period that the IDR value for the CPROP

salt had changed significantly. A closer inspection of the images in Figure 6 explained this phenomenon. The CPROP image showed wave developments (highlighted by red arrows) at around the 15 min time point to be the potential cause of its highly inflated IDR value. This was observed post IDR run to be caused by a crack in the compact potentially caused during media ingress.

This is also highlighted in Figure 7b. The red rectangular insert in Figure 7a also depicts the initial higher IDR values that can alter reliable IDR values thereby highlighting the relevance of the use of the infinite focus variation microscope. A slight decrease in IDR over time with this imaging technique and the shape of the IDR plots as seen in Figure 7 have been observed by other authors and could account for some of the differences in values between the 10 min and 30 min time points (Hulse et al., 2012; Østergaard, 2018). This work therefore brings to light the fact that the actual disc surface in the IDR runs may not be a **uniform** smooth surface as thought when geometric assessment of the surface area for IDR calculations in the traditional way are conducted. Care should therefore be taken to ensure that the surfaces are taken into consideration for future IDR measurements to ensure accurate IDR values are reported.

3.3 Whole dosage dissolution

Figure 8 shows the cumulative release of GEM and its salts with CPROP, CBUT, CPENT and CHEX from the capsules. Ostergaard showed the capabilities of this instrumentation in successfully imaging an anti-diabetic drug on a prototype of this instrument (Østergaard, 2018). Here, the authors have been able to demonstrate for the first time the full capabilities of this instrument in imaging a dosage form (capsule) and understanding its behaviour over a period of 60 min. **It was interesting to note that initial concentration of GEM seemed to be about 4x higher than its salts counterparts. This may be as a result of the actual "content" (amount in weight) within the capsules. The addition of the counterions in the production of the salts meant "more**

sample" being weighed for the capsule filling. The dissolution of the capsule shell would therefore have meant more of the free particles of the GEM drug being exposed to the pH media as compared to the other salts. Over time, the increase in solubility as a result of salt formation may be the driver for improved dissolution of the parent drug. It is also important to note that there was a higher deviation in the GEM drugs full dosage dissolution. The full dosage dissolution showed a trend also in the dissolution of GEM and its salts with CPROP, CBUT, CPENT and CHEX. GEM had an average concentration of 15.99 ± 11.05 μg/mL over the 60 min period. The CPROP, CBUT, CPENT and CHEX salts had average concentrations of 43.93 ± 1.88 μg/mL, 42.71 ± 4.08 μg/mL, 28.09 ± 4.65 μg/mL and 26.20 ± 2.86 μg/mL respectively showing a decrease in dissolution with an increase in the chain length of the counterion. There was a similar **generally trend observed** in the IDR determination. It was also interesting to note the reproducibility of the data with the low standard deviations **for the produced salts**. **The spikes observed at the 45 and 55 min time point for the CBUT salt may have been as a result of aggregated particulates at the bottom of the dosage cell finally getting in full dissolution on some of the triplicate runs causing a higher deviation.**

The full dosage imaging depicted in Figure 9 shows the ability of the instrumentation to image the capsule shell as well as the API present therein. The poor solubility of GEM compared to the salts is evident in Figure 9. After the 60 min time point, about half the capsule shell was still within the capsule holder while this has completely disappeared for the salts. The images also show how the concentration of drug release of the CPROP, CBUT, CPENT and CHEX salts varied over the 60 min time period (depicted by the intense images declining over time). It was observed that this correlated with the chain length of the counterion used and provided a quick visual aid in understanding the effects of the counterion in ranking the salts.

4. CONCLUSIONS

12

Amine salts (CPROP, CBUT, CPENT and CHEX) of GEM, a carboxylic acid drug, was successfully prepared and confirmed using DSC and XRD. IDR results obtained using UV-imaging showed all the salts to have improved values over that of the free acid. Using the UV imaging technique to determine IDR confirmed the impact of surface anomalies, not visible to the eye, on the measured values. The developed interfacial (surface) area ratio (Sdr) obtained from using the focus variation microscope showed a variation of the surface gain for all the salts which could give insights into how the compacts **undergo compression**. The use of various counterions could affect plasticity and therefore elastic recovery and this may also be a contributory factor to surface gain. This however has to be investigated further. Imaging of the powders dissolving from capsule also confirmed the differences in dissolution behaviour. The results suggested an increase in the chain length of the counterion to bring about a decrease in the dissolution of the salts over the free acid i.e. CPROP > CBUT > CPENT > CHEX > GEM. This study is of importance to a formulator as it provides quick insights into how the dissolution of salt forms can be ranked quickly using SDI2 and combining with visual imagery allows for troubleshooting of any anomalies due to surface disparities is adding value to the empirical approach often used in the salt screening process during the preformulation stages.

5. ACKNOWLEDGEMENTS

6. REFERENCES

Adebisi, A.O., Kaialy, W., Hussain, T., Al-Hamidi, H., Nokhodchi, A., Conway, B.R., Asare-Addo, K., 2016a. An assessment of triboelectrification effects on co-ground solid dispersions of carbamazepine. Powder Technol. 292. doi:10.1016/j.powtec.2016.02.008

Adebisi, A.O., Kaialy, W., Hussain, T., Al-Hamidi, H., Nokhodchi, A., Conway, B.R., Asare-Addo, K., 2016b. Solid-state, triboelectrostatic and dissolution characteristics of spray-dried piroxicam-glucosamine solid dispersions. Colloids Surf., B 146, 841–851.

Aigner, Z., Hassan, H.B., Berkesi, O., Kata, M., Eros, I., 2005. Thermoanalytical, FTIR and X-ray studies of gemfibrozil-cyclodextrin complexes. J. Therm. Anal. Calorim. 81, 267–272. doi:10.1007/s10973-005-0777-4

Al-Hamidi, H., Asare-Addo, K., Desai, S., Kitson, M., Nokhodchi, A., 2014. The dissolution and solid-state behaviours of coground ibuprofen–glucosamine HCl. Drug Dev. Ind. Pharm. 1–11. doi:10.3109/03639045.2014.991401

Al-Hamidi, H., Edwards, A.A., Douroumis, D., Asare-Addo, K., Nayebi, A.M., Reyhani-Rad, S., Mahmoudi, J., Nokhodchi, A., 2013. Effect of glucosamine HCl on dissolution and solid state behaviours of piroxicam upon milling. Colloids Surf., B 103, 189–199. doi:10.1016/j.colsurfb.2012.10.023

Al-Hamidi, H., Edwards, A.A., Mohammad, M.A., Nokhodchi, A., 2010a. Glucosamine HCl as a new carrier for improved dissolution behaviour: Effect of grinding. Colloids Surf., B 81, 96–109. doi:10.1016/j.colsurfb.2010.06.028

Al-Hamidi, H., Edwards, A.A., Mohammad, M.A., Nokhodchi, A., 2010b. To enhance dissolution rate of poorly water-soluble drugs: Glucosamine hydrochloride as a potential carrier in solid dispersion formulations. Colloids Surf., B 76, 170–178. doi:10.1016/j.colsurfb.2009.10.030

Ambrus, R., Amirzadi, N.N., Aigner, Z., Szabó-Révész, P., 2012. Formulation of poorly water-soluble Gemfibrozil applying power ultrasound. Ultrason. Sonochem. 19, 286–291. doi:10.1016/J.ULTSONCH.2011.07.002

Amidon, G.L., Lennernäs, H., Shah, V.P., Crison, J.R., 1995. A theoretical basis for a biopharmaceutic drug classification: the correlation of in vitro drug product dissolution and in vivo bioavailability. Pharm. Res. 12, 413–420. doi:10.1023/A:1016212804288

Asare-Addo, K., Conway, B.R., 2017. Chapter 2 Solubility Determinations for Pharmaceutical API, in: Poorly Soluble Drugs: Dissolution and Drug Release. Pan Stanford Publishing, pp. 19–84.

Asare-Addo, K., Šupuk, E., Al-Hamidi, H., Owusu-Ware, S., Nokhodchi, A., Conway, B.R., 2015. Triboelectrification and dissolution property enhancements of solid dispersions. Int. J. Pharm. 485, 306–316. doi:http://dx.doi.org/10.1016/j.ijpharm.2015.03.013

Berge, S.M., Bighley, L.D., Monkhouse, D.C., 1977. Pharmaceutical salts. J. Pharm. Sci. 66, 1–19. doi:10.1002/jps.2600660104

Boetker, J.P., Rantanen, J., Rades, T., Müllertz, A., Østergaard, J., Jensen, H., 2013. A new approach to dissolution testing by UV imaging and finite element simulations. Pharm. Res. 30, 1328–1337. doi:10.1007/s11095-013-0972-0

Chen, Y.M., Lin, P.C., Tang, M., Chen, Y.P., 2010. Solid solubility of antilipemic agents and micronization of gemfibrozil in supercritical carbon dioxide. J. Supercrit. Fluids 52, 175–182. doi:10.1016/j.supflu.2009.12.012

David, S.E., Ramirez, M., Timmins, P., Conway, B.R., 2010. Comparative physical, mechanical and crystallographic properties of a series of gemfibrozil salts. J. Pharm. Pharmacol. 62, 1519–1525. doi:10.1111/j.2042-7158.2010.01025.x

David, S.E., Timmins, P., Conway, B.R., 2012. Impact of the counterion on the solubility and physicochemical properties of salts of carboxylic acid drugs. Drug Dev. Ind. Pharm. doi:10.3109/03639045.2011.592530

Gordon, S., Naelapää, K., Rantanen, J., Selen, A., Müllertz, A., Ostergaard, J., 2013. Real-time dissolution behavior of furosemide in biorelevant media as determined by UV imaging. Pharm. Dev. Technol. 18, 1407–1416. doi:10.3109/10837450.2012.737808

He, Y., Ho, C., Yang, D., Chen, J., Orton, E., 2017. Measurement and Accurate Interpretation of the Solubility of Pharmaceutical Salts. J. Pharm. Sci. 106, 1190–1196. doi:10.1016/J.XPHS.2017.01.023

Hulse, W.L., Gray, J., Forbes, R.T., 2012. A discriminatory intrinsic dissolution study using UV area imaging analysis to gain additional insights into the dissolution behaviour of active pharmaceutical ingredients. Int. J. Pharm. 434, 133–139. doi:10.1016/j.ijpharm.2012.05.023

Korn, C., Balbach, S., 2014. Compound selection for development - Is salt formation the ultimate answer? Experiences with an extended concept of the "100 mg approach." Eur. J. Pharm. Sci. 57, 257–263. doi:10.1016/j.ejps.2013.08.040

Ku, M.S., Dulin, W., 2012. A biopharmaceutical classification-based Right-First-Time formulation approach to reduce human pharmacokinetic variability and project cycle time from First-In-Human to clinical Proof-Of-Concept. Pharm. Dev. Technol. 17, 285–302. doi:10.3109/10837450.2010.535826

Laity, P.R., Asare-Addo, K., Sweeney, F., Šupuk, E., Conway, B.R., 2015. Using small-angle X-ray scattering to investigate the compaction behaviour of a granulated clay. Appl. Clay Sci. 108, 149–164. doi:https://doi.org/10.1016/j.clay.2015.02.013

Niederquell, A., Kuentz, M., 2014. Biorelevant dissolution of poorly soluble weak acids studied by UV imaging reveals ranges of fractal-like kinetics. Int. J. Pharm. 463, 38–49. doi:10.1016/j.ijpharm.2013.12.049

Nielsen, L.H., Gordon, S., Pajander, J.P., Østergaard, J., Rades, T., Müllertz, A., 2013. Biorelevant characterisation of amorphous furosemide salt exhibits conversion to a furosemide hydrate during dissolution. Int. J. Pharm. 457, 14–24. doi:10.1016/j.ijpharm.2013.08.029

Nokhodchi, A., Javadzadeh, Y., Siahi-Shadbad, M.B.-J.M., 2005. The effect of type and concentration of vehicles on the dissolution rate of Compacts., poorly soluble drug (indomethacin) from liquisolid. J Pharm Pharm Sci 8, 18–25.

Østergaard, J., 2018. UV imaging in pharmaceutical analysis. J. Pharm. Biomed. Anal. doi:10.1016/j.jpba.2017.07.055

Østergaard, J., Lenke, J., Sun, Y., Ye, F., 2014. UV Imaging for In Vitro Dissolution and Release Studies: Intial Experiences. Dissolution Technol. 21, 27–38. doi:10.14227/DT210414P27

Pindelska, E., Sokal, A., Kolodziejski, W., 2017. Pharmaceutical cocrystals, salts and polymorphs: Advanced characterization techniques. Adv. Drug Deliv. Rev. 117, 111–146. doi:10.1016/J.ADDR.2017.09.014

Rabinow, B.E., 2004. Nanosuspensions in drug delivery. Nat. Rev. Drug Discov. 3, 785–796. doi:10.1038/nrd1494

Ramirez, M., David, S.E., Schwalbe, C.H., Asare-Addo, K., Conway, B.R., Timmins, P., 2017. Crystal Packing Arrangement, Chain Conformation, and Physicochemical Properties of Gemfibrozil Amine Salts. Cryst. Growth Des. 17, 3743–3750. doi:10.1021/acs.cgd.7b00352

Stahl, P.H., Wermuth, C.G., 2011. Pharmaceutical Salts 2E - Properties, Selection and Use (International Union of Pure and Applied Chemistry), 2nd Editio. ed. WILEY-VCH Verlag GmbH, Weinheim.

Stahl, P.H., Wermuth, C.G., International Union of Pure and Applied Chemistry., 2008. Handbook of pharmaceutical salts : properties, selection, and use, Chemistry International.

Šupuk, E., Ghori, M.U., Asare-Addo, K., Laity, P.R., Panchmatia, P.M., Conway, B.R., 2013. The influence of salt formation on electrostatic and compression properties of flurbiprofen salts. Int. J. Pharm. 458, 118–127. doi:10.1016/j.ijpharm.2013.10.004

Tsutsumi, S., Iida, M., Tada, N., Kojima, T., Ikeda, Y., Moriwaki, T., Higashi, K., Moribe, K., Yamamoto, K., 2011. Characterization and evaluation of miconazole salts and cocrystals for improved physicochemical properties. Int. J. Pharm. 421, 230–236. doi:10.1016/J.IJPHARM.2011.09.034

Ward, A., Walton, K., Box, K., Østergaard, J., Gillie, L.J., Conway, B.R., Asare-Addo, K., 2017. Variable-focus microscopy and UV surface dissolution imaging as complementary techniques in intrinsic dissolution rate determination. Int. J. Pharm. 530, 139–144. doi:10.1016/j.ijpharm.2017.07.053

Williams, H.D., Trevaskis, N.L., Charman, S.A., Shanker, R.M., Charman, W.N., Pouton, C.W., Porter, C.J.H., 2013. Strategies to Address Low Drug Solubility in Discovery and Development. Pharmacol. Rev. 65, 315–499. doi:10.1124/pr.112.005660

Yang, Q., Ren, T., Yang, S., Li, X., Chi, Y., Yang, Y., Gu, J., Hu, C., 2016. Synthesis and Pharmacokinetic Study of Three Gemfibrozil Salts: An Exploration of the Structure-Property Relationship. Cryst. Growth Des. 16, 6060–6068. doi:10.1021/acs.cgd.6b01100

Figure captions

Figure 1. Structure of (a) gemfibrozil, (b) cyclopropylamine, (c) cyclobutylamine, (d) cyclopentylamine and (e) cyclohexylamine

Figure 2. (a) Image of the wire holder designed for holding the capsule, (b) capsule holder inserted into the flow cell to aid acquisition of full dosage imaging

Figure 3. XRPD analysis for the (a) free acid GEM and its salts with (b) CPROP, (c) CBUT, (d) CPENT and (e) CHEX

Figure 4. SEM images of (a) GEM and its salts with (b) CPROP, (c) CBUT, (d) CPENT and (e) CHEX

Figure 5. Surfstand^{TM} images of the representative compacts of **(a)** GEM and its salts with **(b)** CPROP, **(c)** CBUT, **(d)** CPENT and **(e)** CHEX. Images shown from 5-50x magnification to highlight particulates (dashed black circular lines) and impressions from the tooling that could potentially affect IDR measurements.

Figure 6. Surface dissolution imaging of GEM and its salts with CPROP, CBUT, CPENT and CHEX at the 5, 15 and 30 min time points. Red arrow depicts the wave development that resulted in a largely inflated IDR value for the CPROP salt. Note: As discussed earlier, IDR was taken after the 5 min time point only

Figure 7. IDR as a function of time for the GEM and its salts with CBUT, CPENT and CHEX (b) IDR of the CPROP salt. The unpredictability and large variations were due to wave developments as a result of a crack in the surface of the compact after 10 min that was observed post IDR run Note: IDR data was reported after the 5 min mark only. Red insert on Figure 6a is to elaborate the differences or relatively higher IDR values possibly due to drug/salt dust or particulates being on the surfaces of the compacts produced at early time points. Purple line insert in Figure 6b around

the 11 min mark indicates where the surface crack on the compact of CPROP might have occurred to cause further wave developments and thereby erratic IDR measurements

Figure 8. Cumulative amount of GEM and its salts with CPROP, CBUT, CPENT and CHEX released over 60 min using the whole dosage cell inserted in the figure. **The whole dosage form contains 150 mg of GEM powder as from the supplier or 150 mg GEM content from the four salts formulated in a size 0 hard gelatine capsules.**

Figure 9. Full dosage imaging of GEM and its salts with CPROP, CBUT, CPENT and CHEX over the 60 min period. **The whole dosage form contains 150 mg of GEM powder as from the supplier or 150 mg GEM content from the four salts formulated in a size 0 hard gelatine capsules.**

Figures
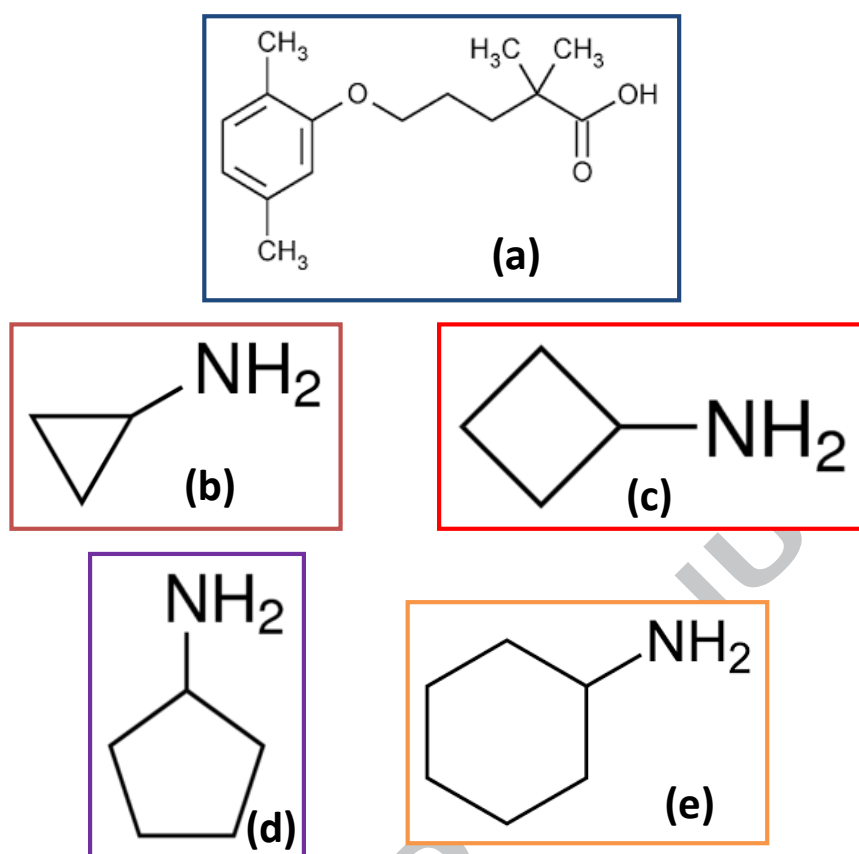
Figure 1.
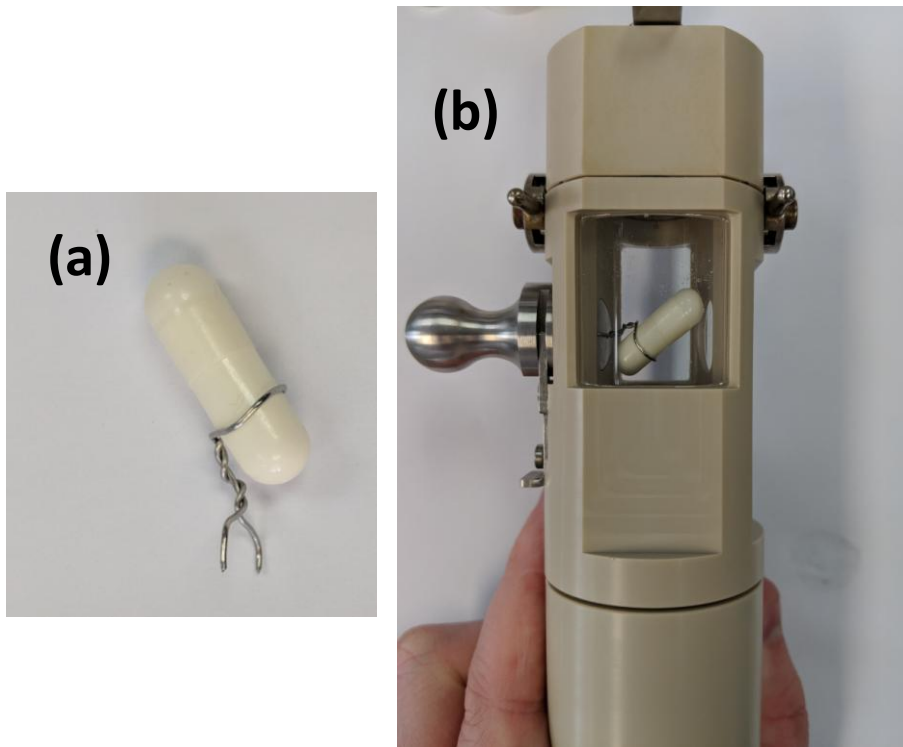
Figure 2.

Figure 3.

Figure 4.

CBUT 5x	CBUT 10x
(c)	

CBUT 20x	CBUT 50x

CPENT 5x	CPENT 10x
(d)	

CPENT 10x	CPENT 50x

Figure 5.

Drug	5 min	15 min	30 min
GEM			
CPROP			
CPENT			
CBUT			
CHEX			
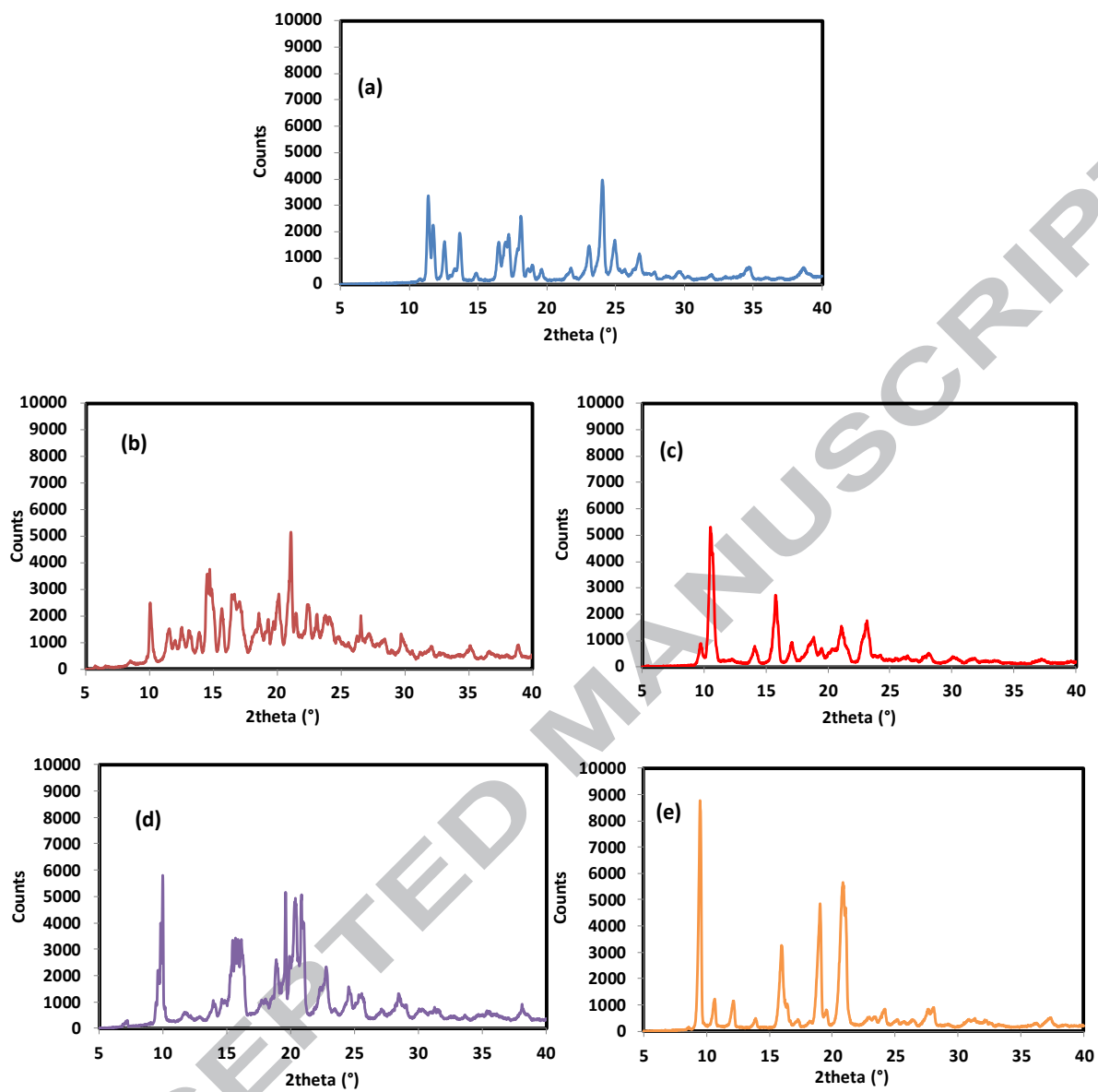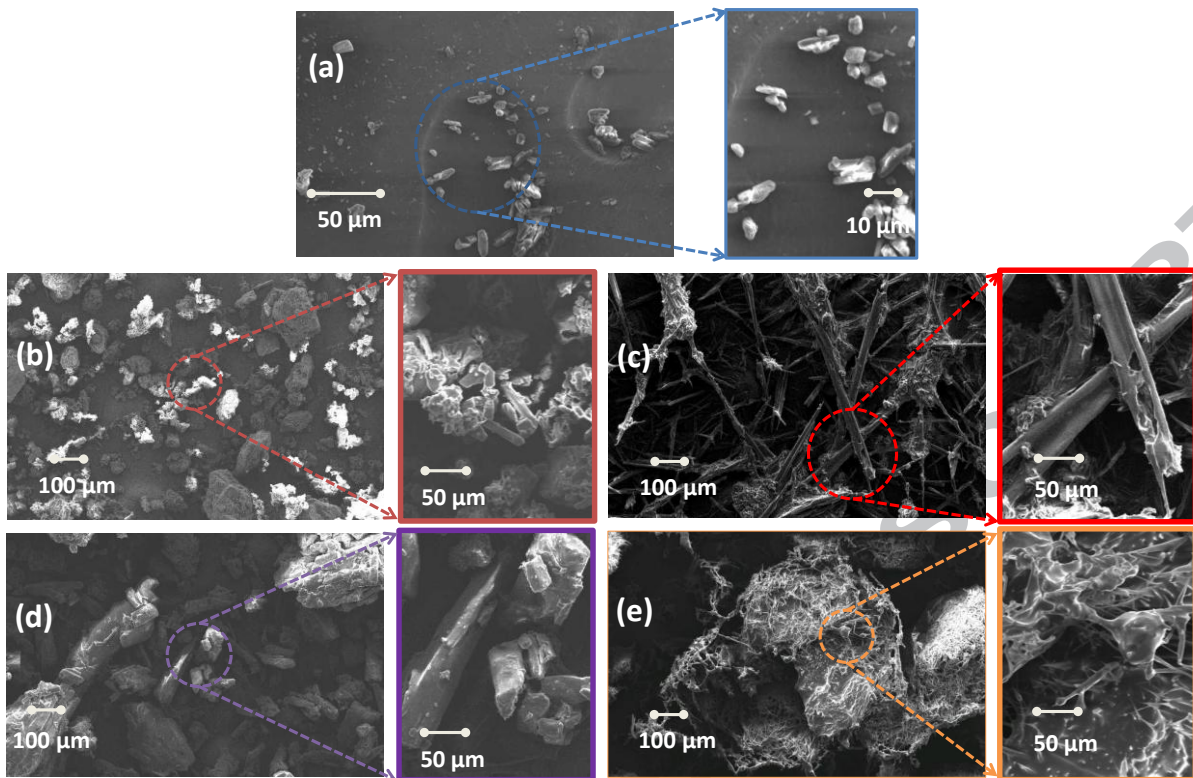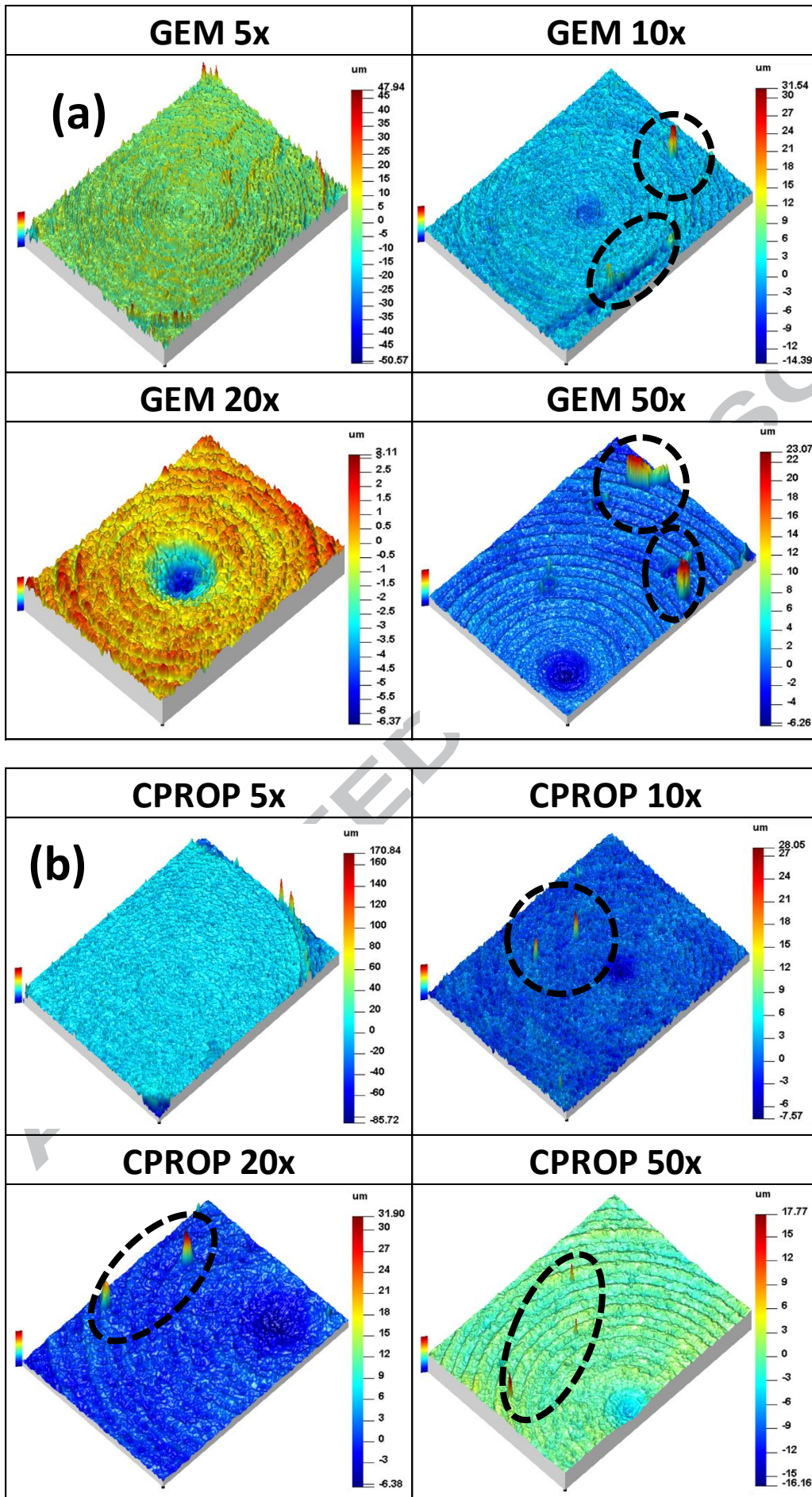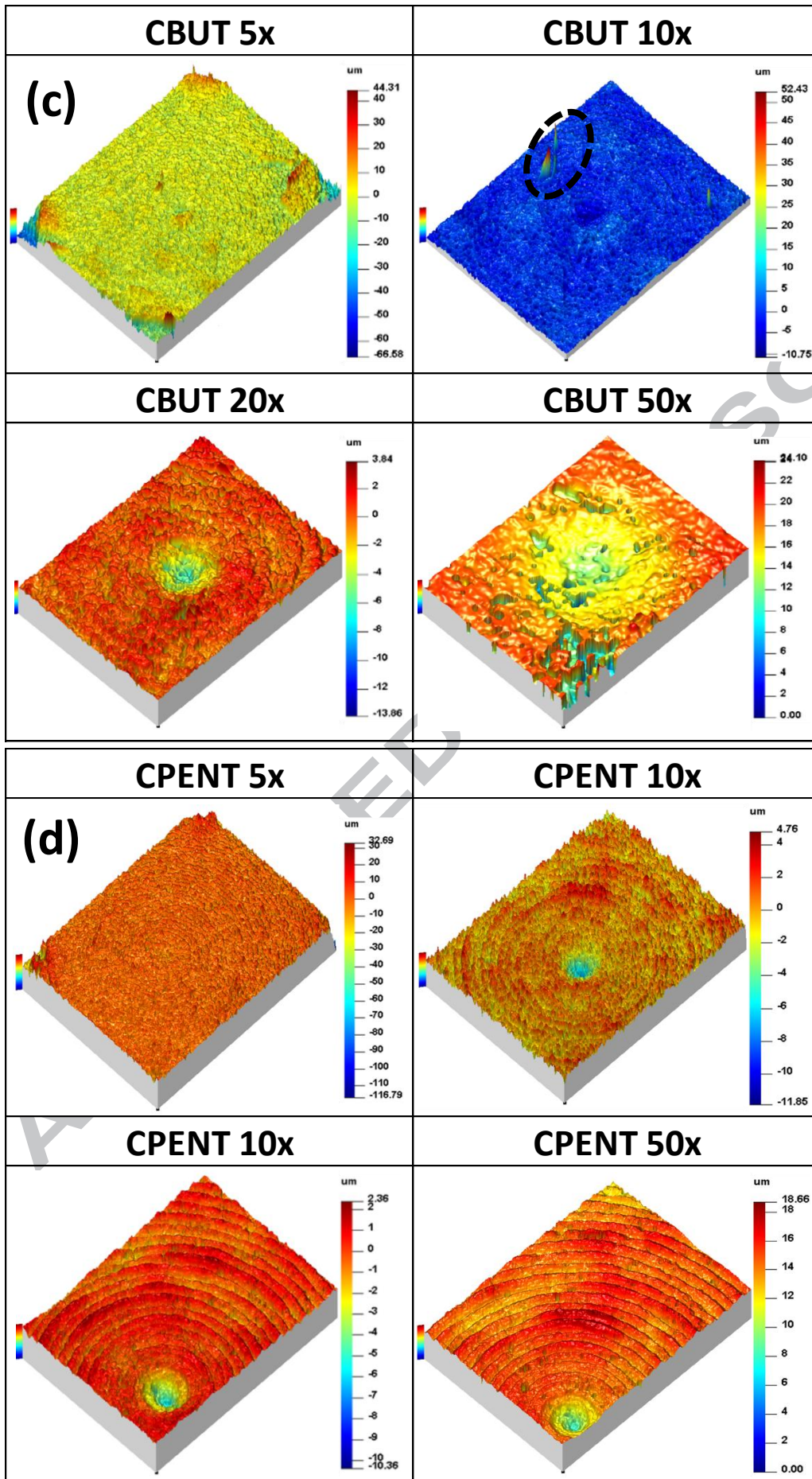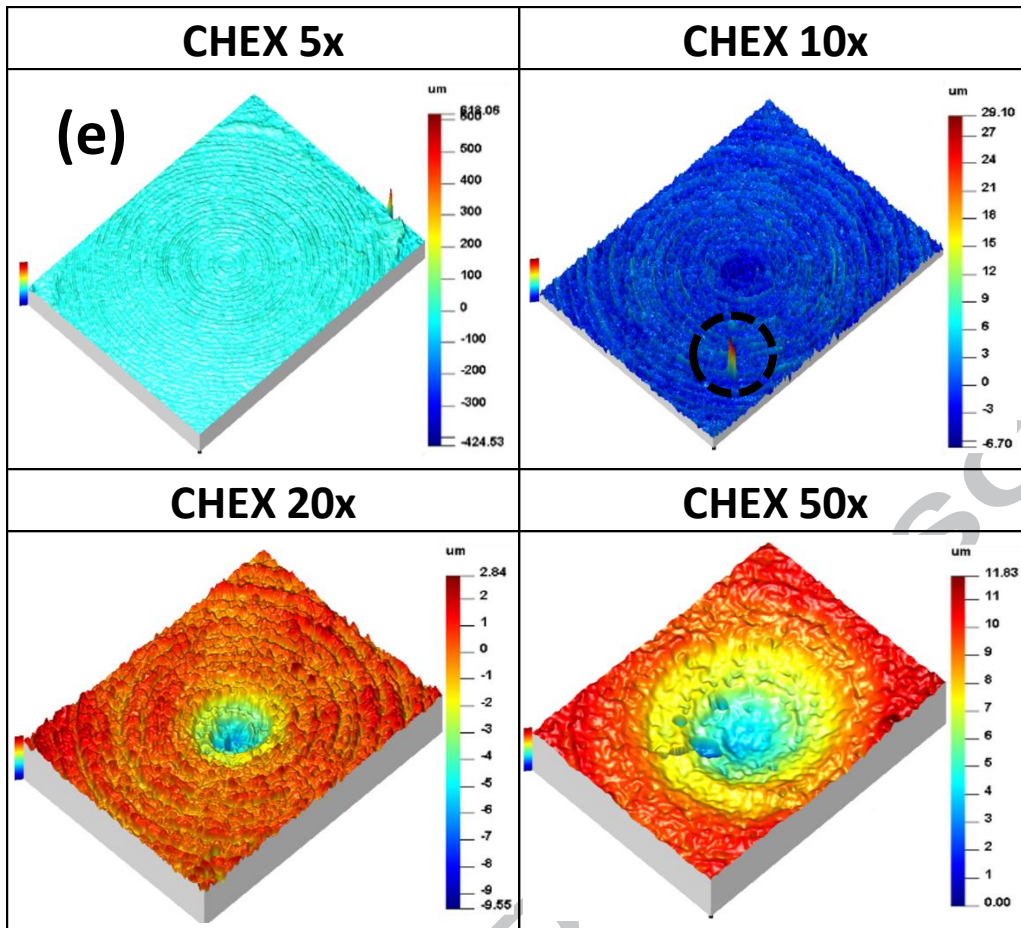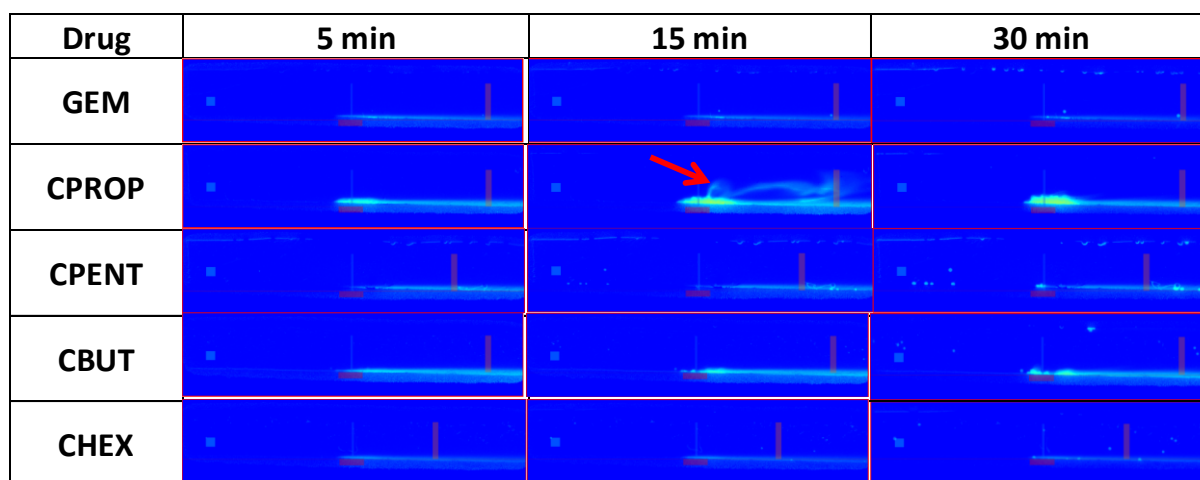
Figure 6.

Figure 7.

Figure 8.

Drug	1 min	3 min	5 min	10 min	30 min	60 min
GEM						
CPROP						
CPENT						
CBUT						
CHEX						
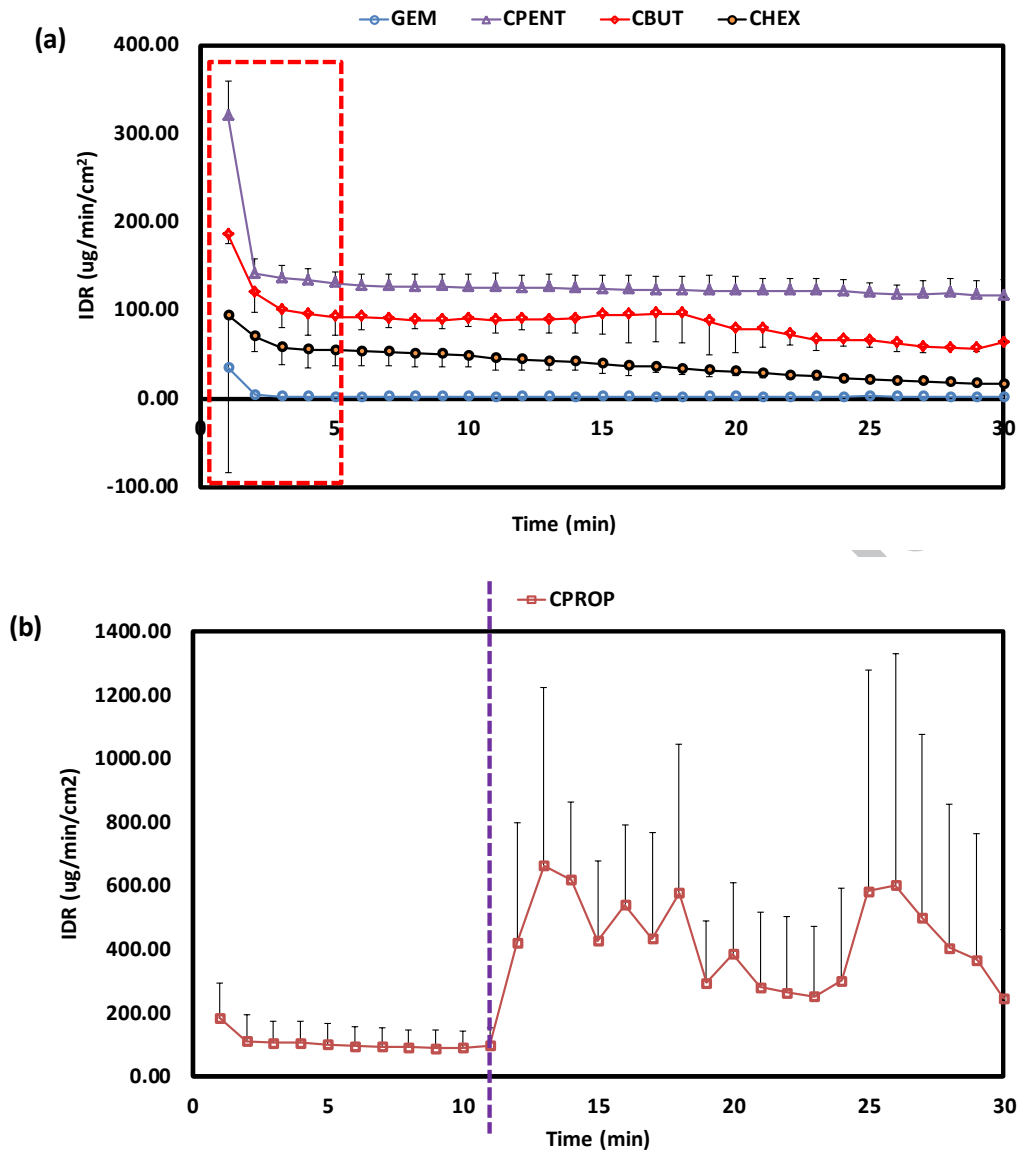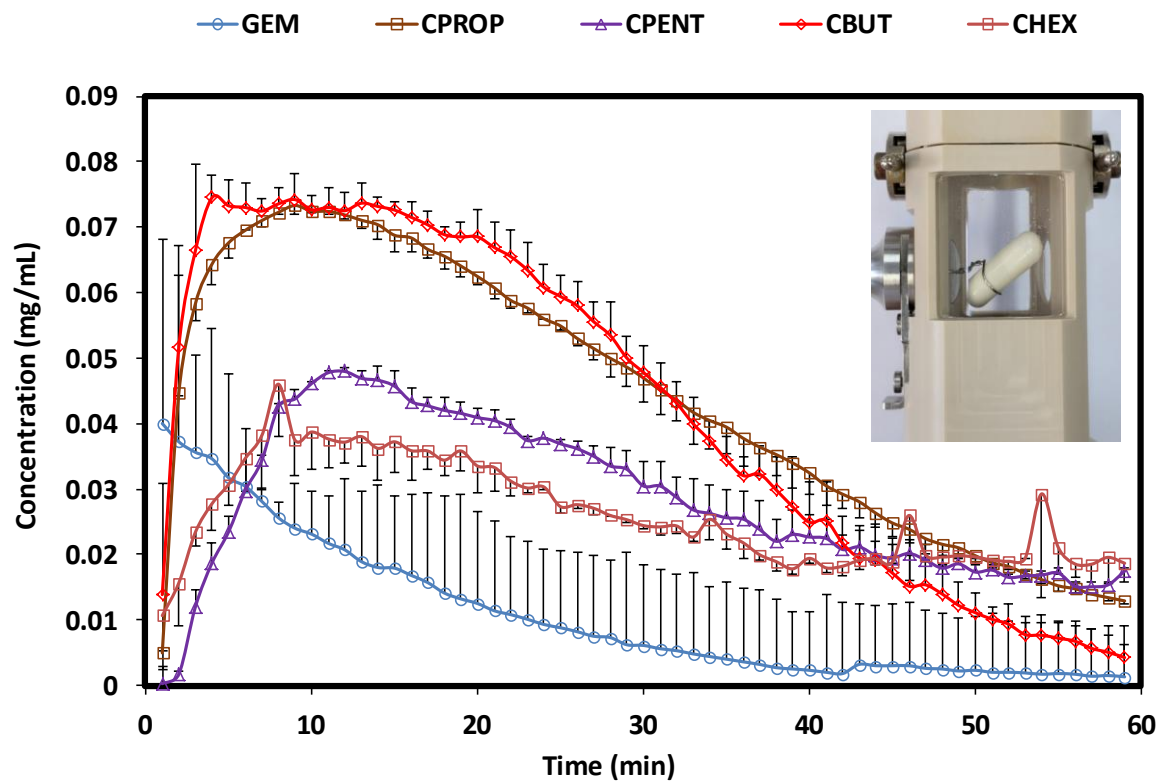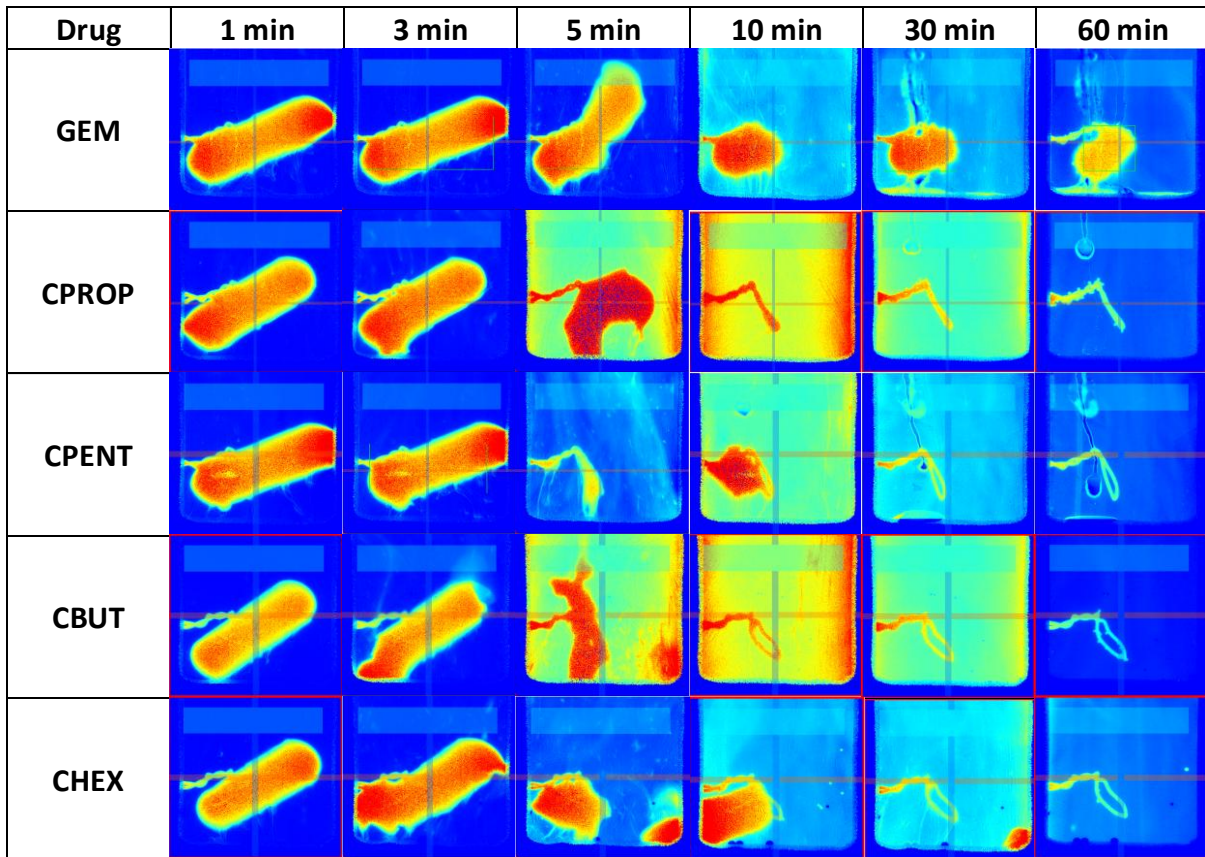
Figure 9.

Tables

Table 1. Melting points, intrinsic dissolution rates and developed interfacial (surface) area ratio for

GEM and CPROP, CBUT, CPENT and CHEX salts

Drug	Melting point (°C)	IDR (µg/min/cm2)*	IDR (µg/min/cm^2)**	Sdr (%)
GEM	60.3	2.01 ± 0.39	2.00 ± 0.38	10.49
CPROP salts	79.9	93.17 ± 4.02	333.78 ± 189.26$^\$$	9.99
CBUT salts	105.0	91.63 ± 2.12	81.43 ± 13.89	4.82
CPENT salts	101.9	127.61 ± 1.87	122.92 ± 3.66	5.87
CHEX salts	134.2	52.97 ± 1.10	35.82 ± 13.00	28.34

Note: * depicts IDR values after 10 min data collection on the SDI2 and ** depicts IDR values after

30 min collection on the SDI2. $ depicts the inflated IDR value for the CROP salt as a result of

wave developments arising from a defect on the surface of the compacts visualised post IDR

analysis.

Highlights

1. **There was a decrease in intrinsic dissolution rate (IDR) with an increase in the chain length of the counterion using UV-imaging**

2. The developed interfacial (surface) area ratio (Sdr) showed significant surface gains for the compacts for IDR determination

3. Loose particulates on surface compacts and observed cracks responsible for inflated IDR values

4. Advanced imaging of surface should be taken into consideration prior IDR determiantion

Graphical abstract

SURSTAND IMAGE

IMPACT ON WHOLE DOSAGE IMAGING

SALT

IMPACT OF SALT ON INTRINSIC
DISSOLUTION RATE